Coherent Neutrino Scattering and Stellar Collapse*

James R. Wilson
Lawrence Livermore Laboratory, University of California, Livermore, California 94550
(Received 24 January 1974)

Freedman has shown that coherency and the neutral current theory of neutrinos imply a scattering cross section for neutrinos off heavy nuclei proportional to the square of the atomic weight. The collapse of an iron-core star produces a hot neutron star surrounded by a thin iron layer. Because of the large scattering rate in the outer layer, neutrinos from the hot neutron core are able to accelerate the iron layer to above escape velocity.

Colgate and White[1] proposed the transport of energy outward by neutrinos during gravitational collapse of a star at the end of its nuclear burning as a nechanism for supernova explosions. Subsequent calculations by Wilson[2] (hereafter designated as I) appeared to rule out this mechanism. Freedman[3] has revived the neutrino explosion mechanism by finding a large coherent neutrino scattering cross section by large nuclei inferred from neutral current theory. Here we investigate the hydrodynamic behavior of stellar collapse, including the neutrino-nuclear scattering as calculated by Freedman.

The model uses the hydrodynamic neutrino transport computer program described in I. In addition to the terms in the neutrino transport equation [Eq. (9) of I] representing the absorption and emission of neutrinos, the term $K_s \times[(4\pi)^{-1}\int F d\Omega - F]$ is added to Eq. (9).

The revised equation (9) for the neutrino energy density F in nonrelativistic form is then (in the present calculations, relativistic effects are small, although the full relativistic equations are still used)

$$\frac{dF}{dt}(\mu,\gamma,R,t)=\frac{\partial F}{\partial t}+\frac{\mu}{R^2}\frac{\partial}{\partial R}(R^2F)+\frac{1}{R}\frac{\partial}{\partial\mu}[F(1-\mu^2)]=K_a\rho(B-F)[1+\exp(-\gamma/T)]+K_s(\tfrac{1}{2}\textstyle\int_{-1}^{1}F d\mu'-F).$$

The first term on the right-hand side represents the absorption and emission of neutrinos and uses the opacity K_a of I with the electron degeneracy factor set equal to 1, except as noted below. The second term represents the effect of elastic scattering and uses the formula from Freedman,[3]

$$K_s=a_0^2(0.9\times10^{-26})\bar{A}\gamma^2\ \mathrm{g/cm^2},$$

where a_0 is an adjustable constant of neutrino theory, $\bar{A}$ is the mean atomic number, and γ is the neutrino energy in keV. The average nuclear mass for zero-temperature material is taken from Negele and Vautherin[4] for densities greater than 4.6×10^{11} g/cm^3 and from Baym, Pethick, and Sutherland[5] for densities less than 4.6×10^{11} g/cm^3. The above data are fitted with a smooth analytical function from a density of 4×10^{10} to a density of 1.4×10^{14}. Below a density of 4×10^{10}, A is taken as 56 for Fe, 28 for Si, 16 for O, and 12 for C. The binding energy E of the nuclei was taken from Negele and Vautherin. A smooth function, again, is used to extend the binding energy from Negele and Vautherin's lowest density point up to Baym, Pethick, and Sutherland's values of binding energy. To take into account the nonzero-temperature effects, the material is assumed to consist of two perfect gases: nuclei of mass A and neutrons. (We ignore intermediate-mass nuclei such as He, which would be present in a narrow region of temperature.) Then a Saha-like equation for equilibrium between nuclei of atomic mass A and neutrons is solved to find the fraction of heavy nuclei, f:

$$\frac{(1-f)^A}{f}=\left[\frac{2(2mkT)^{3/2}}{nh^3}\right]^{A-1}\frac{e-AE/kT}{A^{5/2}}.$$

The $\bar{A}$ as a function of density calculated using this procedure is shown in Fig. 1 for several temperatures. The average nuclear charge is taken from Negele and Vautherin and is assumed to maintain the same ratio to A as the temperature is increased. (The thermal decomposition of neutrons is ignored.) The electron-neutrino absorption opacities of I are calculated using A and Z as found by the above method. The equation of state used is variation III of I with P_1 of Eq. (12) revised to be

$$P_1=\frac{1.7\times10^{13}\rho NT}{1+\exp\{-510/[T+0.258(\rho z)^{1/3}]\}}.$$

Thermonuclear burning of C, O, and Si have

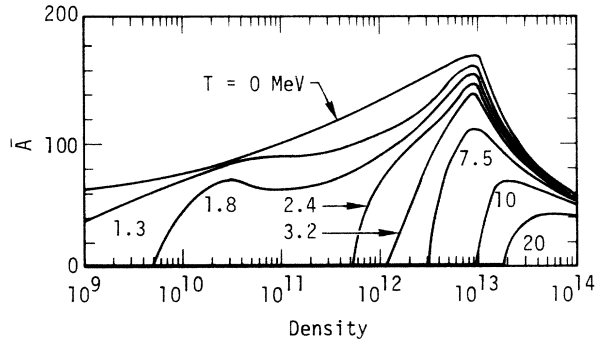

FIG. 1. Average atomic mass versus density for selected temperatures.

been added to the computer program.

A starting configuration was supplied by Barkat using a revised version of the stellar evolutionary program of Rakavy, Shaviv, and Zinamon.[6] This configuration represents the end point of the stellar evolution of a $12M_\odot$ star. Only the inner $1.68M_\odot$, consisting of a $1.49M_\odot$ Fe core surrounded by a thin Si-O layer and a low-density C envelope, is used in the present calculations. The work of Arnett[7] shows that most stars of mass (8 to 30)$M_\odot$ evolve to configurations with (1.4 to 1.5)$M_\odot$ Fe cores.

Three calculations were made starting from the above configuration. In the first calculation, the constant a_0 was set equal to 1.0 and the muon neutrino's opacity was taken as identical to the electron neutrino's opacity. In Fig. 2, the radii of the material shells are plotted as a function of time.

Initially the inner region of the star collapses as a result of the pressure decomposition of iron. When the central density reaches approximately 3×10^{13} g/cm^3, the collapse is halted and an outward shock wave is produced (see Fig. 2). At bounce time, the central temperature is about 30 MeV and the temperature at optical depth 1 is about 5 MeV. The radiation force produced by the emitted neutrinos is then sufficient to push out the high-A material. The outward shock wave also helps start the blowoff process. In this case, a very strong outward explosion was produced in the outer $0.1M_\odot$ of the Fe core. In the outward-moving material, the kinetic energy exceeds the gravitational energy by 10^{51} erg. About $0.1M_\odot$ of material outside of the Fe core was burned to Fe by the end of the computer calculation. At the end of the calculations, only 10^{52} erg of neutrinos have been radiated out of the star. The gravitational binding energy for the neutron star being

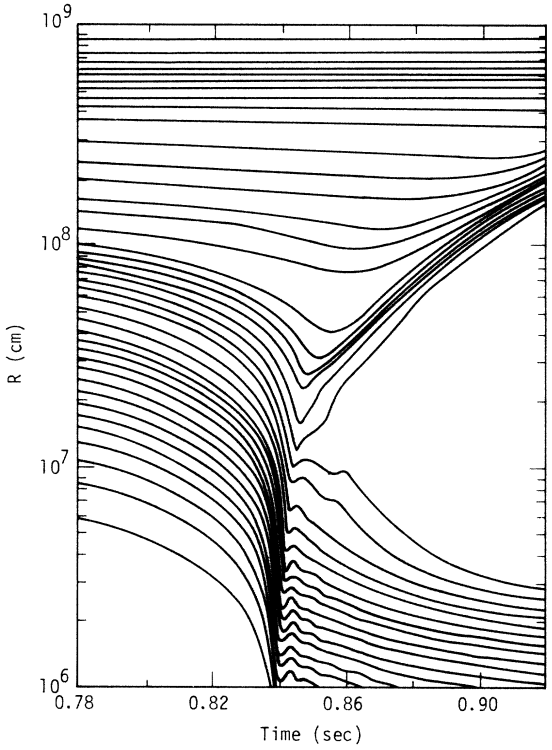

FIG. 2. Radius versus time of computed mass points in the star for the calculation with $a_0 = 1$.

formed is about 10^{53} erg. While a great amount of energy is still to be emitted, the optical depth of the expanding layer is already down to 0.1 at the end of the calculation. It is estimated by extrapolation from the end of the calculation that about 2×10^{51} erg of kinetic energy will be developed. The energy deposited will be of the order of v/c times the optical depth times the energy radiated. The velocity v is approximately $0.1c$ so that about 1% efficiency is obtained. The neutrinos leaving the core and scattering off the outward-moving shell have a mean energy of about 20 MeV.

The second calculation was performed using Freedman's recommended value of $a_0 = 0.45$. Again, electron and muon neutrinos were treated identically. In this case, the behavior was much different (Fig. 3). The outer layers are moving out at much less than escape velocity. In the final calculation, illustrated in Fig. 4, a_0 was taken as 0.45, but the absorption opacity for muon neutrinos was the same as in I. In this case, a mild explosion resulted with an ejected energy of approximately 10^{50} erg. The muon neutrinos cannot have this low an opacity consistent with neutral currents, but this calculation was made as

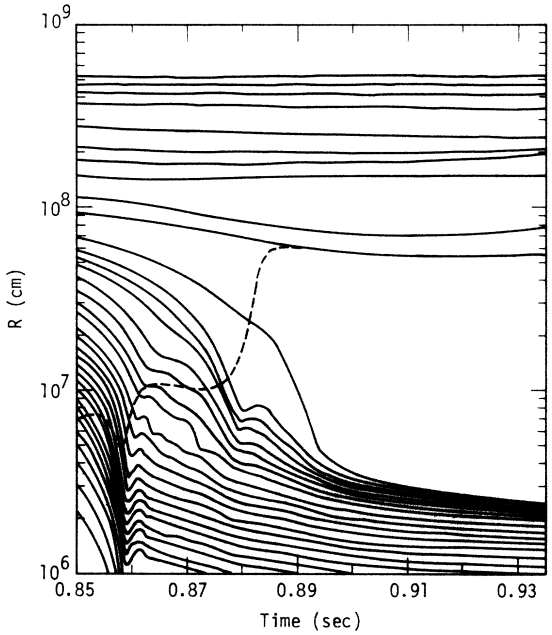

FIG. 3. Radius versus time of mass points in the star for calculation with $a_0 = 0.45$. Dashed curve is the boundary between $\bar{A} \approx 50$ and $\bar{A} = 1.0$.

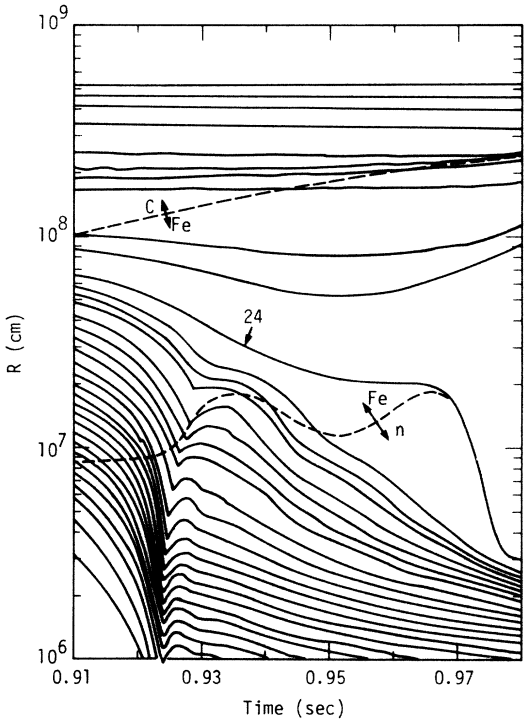

FIG. 4. Radius versus time of mass points in the star for calculation with $a_0 = 0.45$ and old absorption opacity for muon neutrinos. Dashed lines are the boundaries of the region with $\bar{A} \approx 50$.

an extreme example of muon-electron neutrino differences.

The outward motion is produced predominantly by the radiation-pressure force of the neutrinos emitted by the hot neutron core scattering on the iron envelope. In the last two calculations the radiation force is almost equal to the gravitational force in the iron zones. Note in Fig. 4 how zone 24 falls in rapidly when it decomposes from iron to neutrons. The luminosity of the core in the first two examples rises to about 2×10^{54} and remains near that value for the rest of the calculation. The luminosity is about 50% higher for the third example at the end of the calculation.

The star density of the initial configuration was multiplied by 0.9 and 1.1, new initial equilibrium temperatures were found, and the collapse calculations were repeated with the second of the above neutrino opacity options. The results were not significantly altered.

We conclude that the principal uncertainty as to whether the present model provides an adequate model for supernova is the neutrino opacity. In particular, it is the ratio of the opacity in the outer layers relative to the opacity in the core. The absorption opacity of I was used because cross sections for all the reactions are not available and the new values for absorption should not be as grossly different as are the scattering cross sections. It has been pointed out[8] that the treatment of the absorption opacity is naive, in particular the setting of ν_μ opacity equal to ν_e opacity. Since the model is so marginal, these calculations only demonstrate the possibility of this supernova mechanism and indicate the need for a more careful treatment of neutrino interactions and equation of state.

The author would like to thank S. Weinberg for suggesting the possible importance of neutral current effects in stellar collapse, J. Katz for calling attention to the significance of Freedman's work, Z. Barkat for supplying precollapse stellar models, and R. Schwartz for discussions.

*Work performed under the auspices of the U. S. Atomic Energy Commission.

[1]S. A. Colgate and R. H. White, Astrophys. J. 143, 626 (1966).

[2]J. R. Wilson, Astrophys. J. 163, 209 (1971).

[3]D. Z. Freedman, NAL Report No. Pub-73/76-THY, 1973 (unpublished).

[4]J. W. Negele and D. Vautherin, Nucl. Phys. A207, 298 (1973).
[5]G. Baym, C. Pethick, and P. Sutherland, Astrophys. J. 170, 299 (1971).
[6]G. Rakavy, G. Shaviv, and Z. Zinamon, Astrophys. J. 150, 131 (1967).
[7]D. Arnett, in *Explosive Nucleosynthesis*, edited by D. Arnett and D. Schramm (Univ. of Texas Press, Austin, Tex., 1973), p. 236.
[8]S. Bludman, private communication.

Structure in the $\omega\pi\pi$ System at the A_2 Mass Region

U. Karshon, G. Mikenberg, S. Pitluck, Y. Eisenberg, E. E. Ronat, A. Shapira, and G. Yekutieli
Department of Nuclear Physics, Weizmann Institute of Science, Rehovot, Israel
(Received 28 January 1974)

Evidence is presented for an enhancement in the $\omega\pi\pi$ mass spectrum at the A_2 mass region in π^+p interactions at 5 GeV/c. Assuming this effect to be the A_2, we calculate the decay rate relative to the $\rho\pi$ decay mode and obtain the results 0.29 ± 0.08 and 0.10 ± 0.04 for the two final states $A_2^0\Delta^{++}$ and A_2^+p, respectively. Possible explanations of the discrepancy between these numbers are suggested.

Some evidence has been recently presented for the possible decay of the A_2 meson into $\omega\pi\pi$,[1-4] in either the neutral or charged mode. In this note we present results on both decay modes observed in the study of the final states $A_2^0\Delta^{++}$ and A_2^+p in the reactions

$$\pi^+p\to\pi^+p\pi^+\pi^-\pi^0, \quad (1)$$

$$\pi^+p\to\pi^+p\pi^+\pi^-\pi^+\pi^-\pi^0, \quad (2)$$

$$\pi^+p\to p\pi^+\pi^+\pi^-, \quad (3)$$

$$\pi^+p\to p\pi^+\pi^+\pi^-(\mathrm{MM}),\ (\mathrm{MM})\geq 2\pi^0, \quad (4)$$

at 4.93 GeV/c. The data come from a complete subsample of ~320 000 pictures, which is ~40% of the final sample of a high-statistics experiment taken at the Stanford Linear Accelerator Center 82-in. hydrogen bubble chamber. More experimental details are presented elsewhere.[5]

In Fig. 1(a) we present the $\pi_2^+\pi^-\pi^0$ mass distribution of Reaction (1) for events having $M(p\pi_1^+)$ in the Δ^{++} region (1.16–1.28 GeV). In Fig. 1(b) the plot of $M(\pi^+\pi^-\pi^0)$ in the final state $\Delta^{++}\pi^+\pi^-\pi^+\pi^-\pi^0$ of Reaction (2) with the same Δ^{++} cut shows strong ω production. Defining "ω events" by the

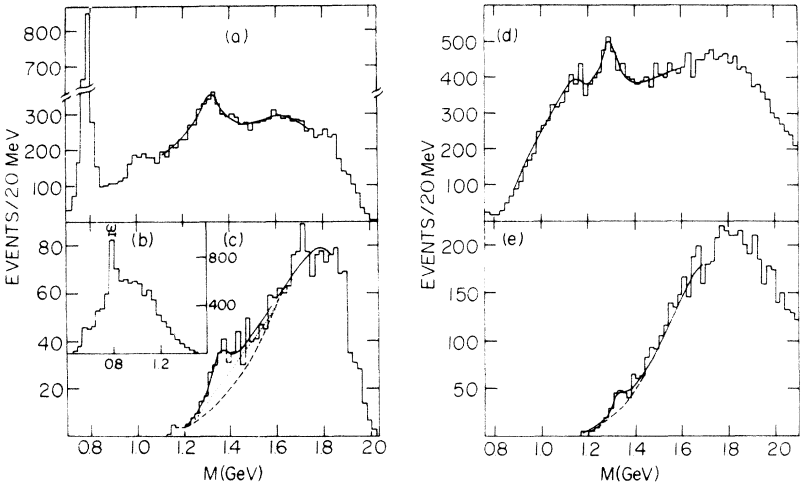

Fig. 1. (a) $M(\pi^+\pi^-\pi^0)$ in the reaction $\pi^+p\to\Delta^{++}\pi^+\pi^-\pi^0$. The curve is the best fit to A_2^0 and hand-drawn background. (b) $M(\pi^+\pi^-\pi^0)$ in the reaction $\pi^+p\to\Delta^{++}\pi^+\pi^+\pi^-\pi^-\pi^0$ (four combinations per event). (c) $M(\omega\pi^+\pi^-)$ in the reaction $\pi^+p\to\Delta^{++}\omega\pi^+\pi^-$. The solid curve is the best fit to A_2^0 and phase space. The background in the A_2^0 region is described by two extremes: The dashed curve is pure phase space (fit 1 in Table I) and the dotted curve is a hand-drawn straight line (fit 4 in Table I). (d) $M(\pi^+\pi^+\pi^-)$ in Reaction (3). The curve is the best fit to A_1^+, A_2^+, and hand-drawn background. (e) $M(\omega\pi^+\pi^0)$ in Reaction (4) with cuts to enhance the ω as described in text. The solid curve is the best fit to A_2^+ and phase space. The dashed curve is phase space in the A_2^+ region.